BUREAU INTERNATIONAL DES POIDS ET MESURES

On-site comparison of Quantum Hall Effect resistance standards of the PTB and the BIPM

· · · Ongoing key comparison BIPM.EM-K12 · · ·

Report on the May 2025 on-site comparison Final report, October 2025

Pierre Gournay*, Benjamin Rolland*,
Mattias Kruskopf**, Eckart Pesel**, Johanna Lengsfeld**, Dinesh K. Patel**

* Bureau International des Poids et Mesures (BIPM)

** Physikalisch-Technische Bundesanstalt (PTB), Germany



1. Introduction

The ongoing on-site comparison BIPM.EM-K12 is part of the BIPM program implemented to verify the international coherence of primary resistance standards. It allows National Metrology Institutes (NMIs) to validate their implementations of the Quantum Hall Effect (QHE) for dc resistance traceability by comparison to the reference maintained at the BIPM.

In this comparison, the value of a 100 Ω standard resistor, calibrated using the NMI's quantum Hall resistance standard (QHRS), is compared with the calibration value of the same resistor obtained by the BIPM using its own transportable QHRS. This comparison is completed by measuring two ratios, $100~\Omega/10~\mathrm{k}\Omega$ and $100~\Omega/1~\Omega$, providing a test of resistance scaling across the central resistance range.

The comparison program BIPM.EM-K12 started in 1993. A first series of five comparisons was carried out from this date until 1999. After a suspension period, the comparison program was resumed in 2013. Since then, eight comparisons have been successfully completed whose results may be consulted on the webpage of the BIPM Key Comparison Data Base (KCDB) [1].

In May 2025 a new BIPM.EM-K12 comparison was carried out at the Physikalisch-Technische Bundesanstalt (PTB), Germany. It was the third time the PTB participated in this ongoing comparison. Previous comparisons were carried out in 1996 and 2013.

For the first time in this key comparison program, the ohm realized from the GaAs-based QHRS of the BIPM was compared to that realized using both GaAs- and graphene-based QHRS of the PTB. This additional comparison measurement is intended to provide further validation of the equivalence between these two types of QHRS and thus confirms the possible use of graphene-based QHRS as a primary standard for realizing the ohm under relaxed experimental conditions (typically 5 T and 4.2 K).

The following sections present the principle of the comparison measurements, the measuring systems being compared and the comparison measurement results.

2. Principle of the comparison measurements

The ohm can be realized from the QHE routinely with an accuracy of the order of 1 part in 10^9 or better. The present comparison is performed on-site in order to eliminate the limitation of transporting transfer resistance standards between the BIPM and the participating institute, which would otherwise result in an increase of the comparison uncertainty by at least a factor of 10.

To this end, the BIPM has developed a complete transportable system that can be operated at the participant's facilities to realize the ohm from a QHE reference at $100~\Omega$ and scale this value to $1~\Omega$ and $10~k\Omega$ (meaning that not only the QHE systems are covered in this comparison but also the scaling devices).

Practically, the comparison comprises three stages schematized in Figure 1:

(i) The calibration of a 100 Ω standard resistor in terms of the ohm realized from the QHE based standards of the PTB and the BIPM. In both of these institutes, the practical realization of the ohm was realized in a manner consistent with the SI Brochure – 9th edition (2019) – Appendix 2 [2]. As recommended in this document, the value of the von Klitzing constant $R_{\rm K}$ = 25 812.807 459 3045 Ω was used (truncated value of h/e^2 with h and e the Planck constant and the elementary charge, respectively). The relative difference in the calibrated values of the standard resistor of nominal value 100 Ω is expressed as ($R_{\rm PTB}$ - $R_{\rm BIPM}$)/ $R_{\rm BIPM}$ where $R_{\rm BIPM}$ and $R_{\rm PTB}$ are the values attributed to $R_{100\Omega}$ by the BIPM and PTB, respectively.

- (ii) The scaling from 100 Ω to 10 k Ω , through the measurement of the ratio $R_{10\text{k}\Omega}/R_{100\Omega}$ of the resistance of two standards of nominal value 10 k Ω and 100 Ω . The relative difference in the measurement of this ratio, hereinafter referred to as K1, is expressed as $(K1_{\text{PTB}} K1_{\text{BIPM}})/K1_{\text{BIPM}}$ where $K1_{\text{BIPM}}$ and $K1_{\text{PTB}}$ are the values attributed to K1 by the BIPM and the PTB, respectively.
- (iii) The scaling from $100~\Omega$ to $1~\Omega$, through the measurement of the ratio $R_{100\Omega}/R_{1\Omega}$ of the resistance of two standards of nominal value $100~\Omega$ and $1~\Omega$. The relative difference in the measurement of this ratio, hereinafter referred to as K2, is expressed as $(K2_{PTB} K2_{BIPM})/K2_{BIPM}$ where $K2_{BIPM}$ and $K2_{PTB}$ are the values attributed to K2 by the BIPM and the PTB, respectively.

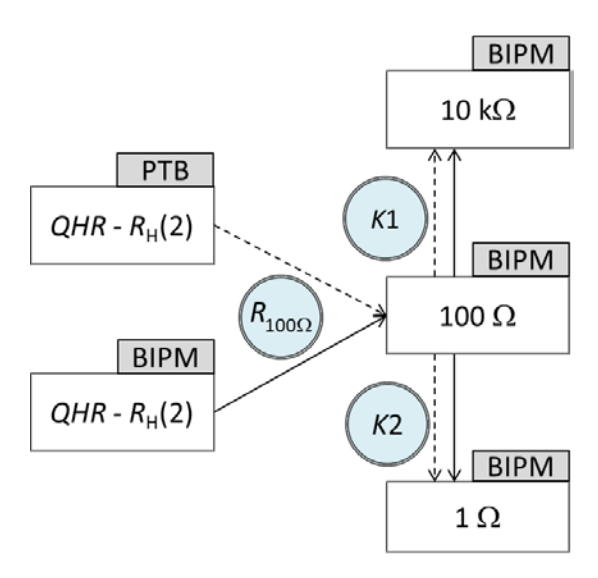


Figure 1: Schematic of the on-site comparison carried out at the PTB in May 2025. Rectangles represent the resistances to be compared, and circles correspond to the resistance $R_{100\Omega}$ or the ratios K1 and K2 to be measured. Solid and dashed arrows stand for the measurements with the 1 Hz bridge of the BIPM or with the CCC bridge of the PTB, respectively.

The resistance value of each of the standard resistors used in this comparison is defined as its five-terminal dc-resistance value 1 . This means, unless otherwise specified, that it corresponds to the dc voltage to current ratio once any thermal EMF across the resistor, particularly those induced by the Peltier effect, have reached a stable value. The influence of the Peltier effect on precision resistance measurements has already been discussed in several papers [3-8], in which an extended description of the observed phenomena is provided (in particular regarding $1\,\Omega$ resistance measurement).

3. The BIPM measurement system and the transfer standards

3.1. Implementation of the QHE

A complete transportable QHE reference [9] has been developed at the BIPM for the purpose of the BIPM.EM-K12 on-site comparison program. It is composed of a compact liquid helium cryostat equipped with an 11.3 T superconducting magnet and a sample space that can be cooled to 1.4 K with the included vacuum pump. The magnet has an additional support at the bottom of the dewar to allow safe transport.

Final report Page 3

-

¹ Ratio of the voltage drop between the high and low potential terminals to the current flowing in the low current terminal, with the case - fifth terminal - maintained at the same potential as the low potential terminal.

The separate sample probe can support two TO-8 mounted quantum Hall devices simultaneously (side by side within the magnet), with guarded wiring for eight terminals on each device. For this comparison, BIPM used GaAs heterostructure devices fabricated by PTB. They show an i=2 plateau centered on typical flux density values between 10 T and 10.5 T, which are well quantified for currents of the order of 50 μ A at 1.4 K. The cryostat and the QHE devices are suitable for a realization of the ohm meeting all the requirements of the CCEM guidelines [10] for a relative standard uncertainty of the order of 1×10⁻⁹.

A transportable resistance bridge is used with the QHE cryostat for the measurement of the different resistance ratios being the subject of the comparison. It is based on a room-temperature low-frequency current comparator (LFCC) operated at 1 Hz (sinusoidal signal), meaning that all resistance or ratio measurements are carried out at 1 Hz by the BIPM during the comparison. That way to proceed is preferable to the transport of the BIPM Cryogenic Current Comparator (CCC) bridge on-site since the 1 Hz bridge is a more rugged instrument, simple to operate, and less sensitive to electromagnetic interference and temperature variations. Furthermore, it provides resolution and reproducibility that are comparable to those achievable with the BIPM CCC bridge. However, the performances of the 1 Hz bridge may possibly depend on the experimental conditions encountered on-site.

The 1 Hz bridge is equipped with two separate LFCCs of ratio 129:1 and 100:1, having turns 2065:16 and 1500:15. The construction and performance of these devices are detailed in [11,12].

3.2. Transfer standards

Four transfer resistance standards were used in the comparison: two with a nominal value of 100 Ω , one with 1 Ω , and one with 10 k Ω . The measurands compared in this exercise are the values assigned by the BIPM and the PTB to one of the two 100 Ω resistors in terms of $R_{\rm K}$, and to the two ratios 100 $\Omega/1$ Ω and 10 k $\Omega/100$ Ω .

The transfer standards were provided by the BIPM. The two $100~\Omega$ standards were a SR102 type resistor from Tegam (s/n: A 2030405SR102) and an HRU-101 type resistor from Alpha Electronics (s/n: F078A). The $10~\mathrm{k}\Omega$ standard was a SR104 type resistor from Tegam (s/n: K 201119630104) and the $1~\Omega$ was a HRU-1R0 type resistor from Alpha Electronics (s/n: F112A). All four resistors were fitted in individual temperature-controlled enclosures held at $25~\mathrm{^{\circ}C}$. The temperature-regulation system can be powered either from the mains or from external batteries.

For each of these standards, the difference between resistance values measured at 1 Hz and at 'dc' is small but not negligible. Therefore, the same applies to the ratios of standards such as K1 and K2. The differences 1 Hz-'dc' for the measurands $R_{100\Omega}$, K1 and K2 were determined at the BIPM prior to the comparison. The 'dc' value was measured with the BIPM CCC whilst the 1 Hz value with the transportable 1 Hz bridge (the same as that used for on-site measurements). The differences are applied as corrections to the measurements performed at 1 Hz meaning that the 1 Hz bridge is used as a transfer instrument referenced to the BIPM CCC.

The frequency corrections (1 Hz-'dc') are reported in Table 1 for $R_{100\Omega}$, K1 and K2. The main possible sources contributing to these corrections are the quantum Hall resistance (QHR), the 1 Hz bridge, the transfer standard itself and possibly the measuring cable. Nevertheless, at 1 Hz, the frequency dependence of the QHR is negligible compared to the comparison uncertainty [13], and the characterization of the bridge provides evidence that its error at 1 Hz is below 1 part in 10^9 . Consequently, the frequency dependence observed is mainly attributed to the resistance standards themselves (including their conditioning).

Resistance or resistance ratio	$100~\Omega$ transfer standard used for the comparison	1 Hz-'dc' correction/10 ⁻⁹	Standard uncertainty/10 ⁻⁹
100 Ω	s/n: A 2030405SR102	6.0	1.0
<i>K</i> 1	s/n: A 2030405SR102	1.0	1.0
K2	s/n: F078A	-4.7	1.5

Table 1: Value of the 1 Hz to 'dc' corrections applied to the BIPM measurements carried out at 1 Hz (Value('dc')=Value(1 Hz)+ Correction). These values are specific to the standards used in this comparison.

For the sake of completeness, it must be noted that the 'dc' resistance value (or ratio) measured with the BIPM CCC bridge results from a current signal driven through the resistors having polarity reversals with a waiting time at zero (36 s) between polarity inversions, cf. Figure 2. The polarity reversal frequency is on the order of 3 mHz (about 340 s cycle period) and the measurements are sampled only during the last 100 s before the change of polarity.

Previous characterization measurements of the $R_{\rm H}(2)/100~\Omega$ (where $R_{\rm H}(2)=R_{\rm K}/2$ corresponds to the value of the QHR for a filling factor i=2) and $10~{\rm k}\Omega/100~\Omega$ ratios have shown that if the polarity reversal frequency is kept below 0.1 Hz, then any effects of settling or ac behaviour remain on the order of 1 part in 10^9 or less. Regarding the $100~\Omega/1~\Omega$ ratio, this is most often not the case due to Peltier effects in the $1~\Omega$ standard.

In order to ensure the best possible comparability of the measurements performed by the BIPM and the participating institute, the measuring system of the latter should be configured to match as closely as possible the reference polarity reversal cycle of the BIPM CCC. In case this is not feasible, a correction must be estimated and applied to the participating NMI's measurements based either on additional characterization of the influence of the polarity reversal rate on the actual measured resistance ratio, or by any other means using the most relevant and reliable information available.

In that respect, in case different current reversal cycles (shape and/or magnitude) would be used by the BIPM and the NMI, an estimation of the difference of the effective powers dissipated in the measured resistance standards should be done and, if necessary, a correction applied considering the power coefficients of those standards.

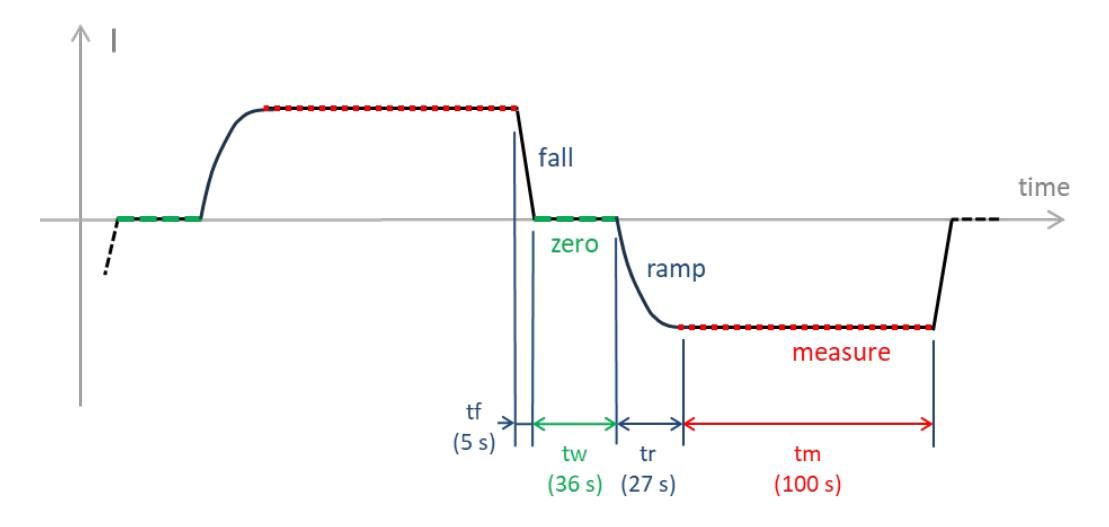


Figure 2: Schematic representation of the reference current cycle with polarity reversals used in the BIPM CCC bridge. Each half-cycle comprises a waiting time at zero current of 36 s, a ramp time of 27 s, a measuring (sampling) time of 100 s and a fall time of 5 s. The complete reversal cycle time is 336 s.

3.3. Uncertainty budget

Table 2 summarizes the BIPM standard uncertainties for the measurement of the 'dc' value of the 100 Ω standard in terms of the von Klitzing constant R_K (as defined section 2), as well as the measurement uncertainties for both the 10 k Ω /100 Ω and 100 Ω /1 Ω ratios (K1 and K2, respectively).

Maggurom ont Dayam etoya	Resistance ratio		
Measurement Parameters	R _H (2)/100 Ω	$10~\mathrm{k}\Omega/100~\Omega$	100 Ω/1 Ω
LFCC ratio	129/1	100/1	100/1
Currents	40 μA/5.16 mA	50 μA/5 mA	0.5 mA/50 mA
Uncertainty contributions (type-B)	Relative standard uncertainties / 10 ⁻⁹		
Imperfect CCC winding ratio	1.0	1.0	1.0
Resistive divider calibration	0.5	0.5	0.5
Leakage resistances	0.2	0.2	-
Noise rectification in CCC	1.0	1.0	1.0
Imperfect realization of the QHR	0.8	-	-
Correction of the 1 Hz-to 'dc' difference	1.0	1.0	1.5
Combined type B standard uncertainty, u _B	2.0	1.8	2.1

Table 2: Contributions to the combined type B standard uncertainty for the 'dc' measurement of the three mentioned resistance ratios at the BIPM.

4. The PTB measurement system

4.1. Implementation of the QHE

The quantum Hall resistance standard is operated in an Oxford Instruments cryomagnet located in laboratory 020 in the Heisenberg-building at PTB Braunschweig, with a maximum achievable magnetic flux density of 12 T. The GaAs-based QHR device (sample P876-21) and the graphene-based QHR device (G1534_F13#6) undergo a characterization procedure to ensure the integrity of the quantized Hall resistance as described in section 5.2.1 and 6.2.1.

4.2. Resistance bridge

The resistance bridge employed by PTB for the comparison is a home-made 14-bit-based CCC bridge. The system is similar to the commercially available 12-bit version [14,15,16] but includes additional windings (in total 19 individual packages), each having between 1 and 8192 turns which can be individually combined to achieve a large variety of winding ratios in the CCC probe.

The current driven through the resistors is reversed periodically as depicted in Figure 3. Table 3 summarizes the timing details of the current reversal cycles which were employed by the PTB during the present comparison measurements.

For the comparison measurements of the ratio $R_{\rm H}(2)/100~\Omega$ and the K1 ratio $10~{\rm k}\Omega/100~\Omega$, a full cycle time of 20 s was used which is the standard cycle used routinely at the PTB. No corrections related to the cycle time were applied to these ratios.

For the K2 ratio $100~\Omega/1~\Omega$, the influence of the full cycle time was investigated for the cycle times 6 s, 10~s, 20~s, 40~s and 340~s as described in detail in Table 3. The reason why the cycle time was varied is that previous investigations found a cycle time dependence, specifically in the K2 ratio $100~\Omega/1~\Omega$, which may result in significant differences when compared against BIPM's CCC bridge operating with a cycle time of about 340~s.

In addition to the three ratios that are typically part of the BIPM.EM-K12 comparison, a direct comparison between the QHR realized in BIPM's system using a GaAs-based device and the QHR realized in PTB's system using a graphene-based device was performed. For the 1:1 comparison, a CCC turn ratio of 4096 to 4096 and the typical cycle time of 20 s were used.

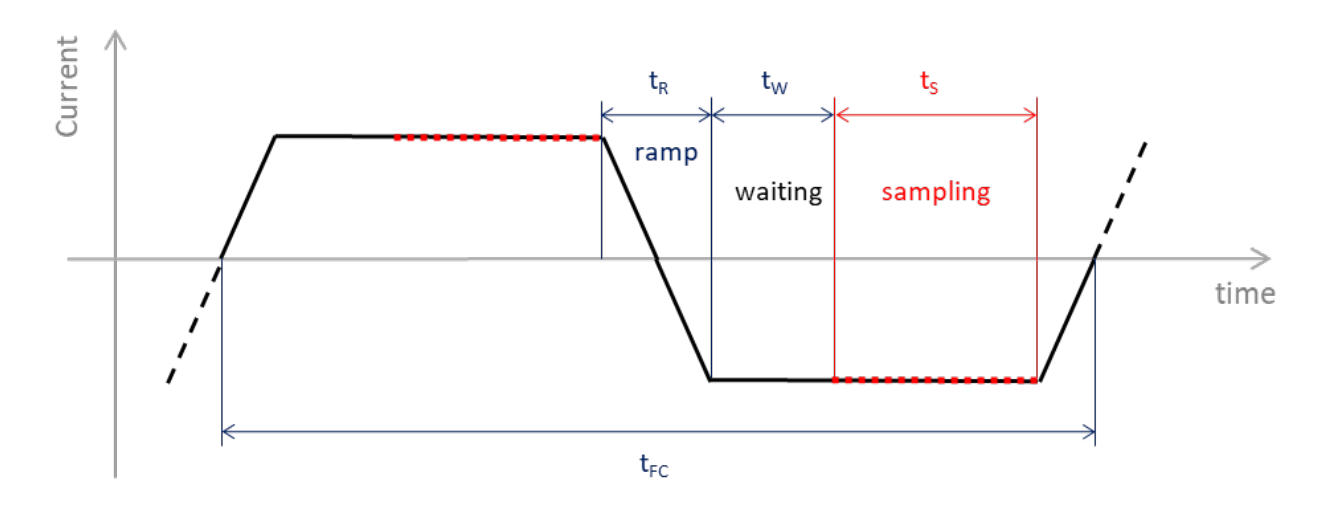


Figure 3: Current reversal timing of the PTB measurement. t_R , t_W , t_S , and t_{FC} are the ramp time, waiting time, sampling time, and full cycle time, respectively.

Cycle time /s	<i>t</i> fc /s	<i>t</i> _R /S	<i>t</i> w /s	<i>t</i> s /s
340	340	0.32	9.84	160
40	40	0.32	9.84	10
20	20	0.32	4.84	5
10	10	0.32	2.24	2.6
6	6	0.32	1.24	1.6

Table 3: Timing details of the current reversal cycles used during $\mathit{K2}$ ratio $100\,\Omega/1\,\Omega$ comparison measurements.

4.3. Measuring environmental conditions

During the whole period of the comparison - 8 to 14 May 2025 - the laboratory maintained an ambient temperature at (22.5 ± 0.5) °C and a relative humidity at (45 ± 5) %. The atmospheric pressure remained within 1005.0 hPa and 1014.5 hPa with a mean value of 1010.8 hPa.

4.4. Uncertainty budget

In Table 4, measurement parameters, typical type A uncertainties as well as the type B uncertainty contributions in the uncertainty budget of PTB's measurements are listed for the mentioned four resistance ratios.

	Resistance ratio			
Measurement Parameters	R _H (2) / 100 Ω	10 kΩ / 100 Ω	100 Ω / 1 Ω	R _H (2)(graph, _{РТВ}) / R _H (2)(GaAs, _{ВІРМ})
Number of turns N_1/N_2	4001/31	4100/41	200/2	4096/4096
Voltage drop $\Delta(I_2R_2)$ in V_{pk-pk} / V	1	1	0.1	1
Compensation ratio <i>k</i>	-1.423 ×10 ⁻²	6.729 ×10 ⁻³	1.7261 ×10 ⁻⁴	0
Correction of $R_{\rm H}(2)$ due to dissipation / 10^{-9}	-0.170 ^(*) -0.244 ^(**)	NA	NA	-0.244 (**)
Duration of individual measurement	20 min	25 min	20 min	30 min
Type A uncertainty contribution	Relative standard uncertainties / 10 ⁻⁹			
Standard deviation for duration of individual measurement	0.168 (*) 0.180 (**)	0.694	0.740	0.179
Type B uncertainty contributions	Re	elative stand	ard uncerta	inties / 10 ⁻⁹
CCC principal windings ratio	0.058	0.058	0.058	0.058
Compensation ratio k	0.021	0.009	0.005	0
Detector linearity + SQUID down-mixing	0.011	0.009	0.016	0.010
Voltage drop Δ(IR) measurement	0.002	0.004	<0.001	<0.001
Leakage resistances	0.006	0.006	<0.001	0.075
Correction of $R_{\rm H}(2)$ due to dissipation	0.137 ^(*) 0.070 ^(**)	NA	NA	0.070 (**)
Combined type B standard uncertainty, $u_{\rm B}$	0.151 (*) 0.094 (**)	0.060	0.060	0.118

Table 4: Measurement parameters, type A and type B uncertainty contributions (k=1) to the uncertainty budget of the measurements by PTB. The indices (*) and (**) indicate the values corresponding to the two cases using either PTB's GaAs-based(*) or graphene-based(**) device, respectively. The stated type A uncertainties correspond to the first comparison measurement (of five) of each ratio and thus represent typical values. Due to small differences in the dissipation in both QHR devices used by PTB, the applied corrections and corresponding type B uncertainties are provided as indicated by the indices (*) and (**). The choice of a single-turn auxiliary winding to implement the compensation for balancing the CCC bridge is common to all configurations.

5. Measurement of the 100 Ω transfer standard in terms of $R_H(2)$ using GaAs-based QHE devices

5.1. BIPM measurements

5.1.1. Preliminary tests

The GaAs-based quantum Hall device used by the BIPM for this comparison is of PTB-type. It was characterized at BIPM prior to the comparison and has shown equivalence with a LEP514-type device within the uncertainty of measurement of the BIPM QHE system. It was operated on the i=2 plateau at a temperature of 1.4 K and with a rms current of 40 μ A.

The magnetic flux density corresponding to the center of the plateau was determined by recording the longitudinal resistance Rxx as a function of magnetic flux density and was found to be about 10.5 T. The two-terminal Hall resistance of the four-terminal pairs device was checked before and after each series of measurements, showing that the contact resistance was smaller than a few ohms (and in any case not larger than 3 Ω - considering the 5 Ω resolution of the handheld multimeter used and the resistance of the two device connecting wires of approximately 1.2 Ω each).

The absence of significant longitudinal dissipation along both sides of the device was tested as described in [10] section 6.2, by combining the measurements obtained from four different configurations of the voltage contacts (opposite and diagonal configurations between the voltage contact pairs at both sides of the device). The absence of dissipation was demonstrated within less than 5×10^{-10} in relative terms with a standard uncertainty of the same order. No correction was applied to compensate for possible imperfect quantization, but an uncertainty component for imperfect QHR realization is considered in Table 2. The difference between measurements made using opposite (orthogonal) pairs of voltage contacts in the center and on either side of the sample was also found to be uniform within less than 5×10^{-10} .

The series of measurements performed subsequently for the purpose of the comparison were taken from the central pair of contacts only.

5.1.2. BIPM results

On May 8, 2025, the QHE systems of the BIPM and PTB were operational to perform the $100\,\Omega$ comparison based on $R_{\rm H}(2)$. The $100\,\Omega$ standard (Tegam s/n: A 2030405SR102) was connected alternately to the BIPM and PTB bridges for a total of five BIPM measurements interleaved with five PTB measurements. After each change, at least 10 minutes were allowed for thermal stabilization of the connections, with measurement current applied.

As mentioned earlier, a rms current of 40 μ A was applied to the BIPM quantum Hall standard. The current in the 100 Ω transfer standard was therefore 5.16 mA, which corresponds to a Joule heating dissipation of about 2.66 mW.

The values of the 100 Ω standard measured by the BIPM at 1 Hz are shown in Table 5 as well as the 'dc' corrected values (using the 1 Hz-'dc' correction from Table 1). Both are expressed as the relative difference from the 100 Ω nominal value: ($R_{\rm BIPM}/100~\Omega$) - 1. Each of the measurements reported in the table is the average value of a series of five individual measurements and corresponds to a total measurement time of about 19 minutes.

The resistance value R_{BIPM} reported below corresponds to the mean of the corrected measurements carried out by the BIPM on May 8, 2025:

Mean value: $R_{\text{BIPM}} = 100 \times (1 - 0.155 \, 8 \times 10^{-6}) \, \Omega$

Relative standard uncertainty: $u_{\text{BIPM}} = 2.1 \times 10^{-9}$

where u_{BIPM} is calculated as the root sum square of $u_{\text{A}} = 0.6 \times 10^{-9}$ (Table 5) and $u_{\text{B}} = 2.0 \times 10^{-9}$ (Table 2).

	$(R_{\rm BIPM}/100~\Omega)$ -1 /10 ⁻⁶		Dispersion
Time	1 Hz measurements	'dc' corrected (with 1 Hz-'dc' correction)	/10 ⁻⁶
12:47	-0.162 79	-0.156 79	0.000 72
14:06	-0.161 53	-0.155 53	0.000 35
15:21	-0.161 03	-0.155 03	0.000 53
16:37	-0.16186	-0.155 86	0.000 41
17:44	-0.161 72	-0.155 72	0.000 38
	Mean value	-0.155 78	
	Standard deviation, u_A	0.000 57	

Table 5: BIPM measurements of the 100 Ω standard in terms of $R_{\rm H}(2)$ on May 8, 2025. Results are expressed as the relative difference from the nominal 100 Ω value. Each measurement is the average value of a series of five individual measurements. Time corresponds to the starting time of this measurement series and the dispersion to the standard deviation of the mean.

5.2. PTB measurements

5.2.1. Preliminary tests

The probe with the mounted GaAs device P876-21 is cooled from room temperature to 2.2 K with all contacts short-circuited to each other and to the probe housing. After the cooldown is completed, the short-circuit is removed. To start with the characterization, the probe is connected through an eight-pin interface to a PC-controlled measurement setup comprising a precision current source and a nano-voltmeter (Keithley 6220 and 2182, respectively).

The characterization procedure of the QHR device follows the methods described in the established "Revised technical guidelines for reliable dc measurements of the quantized Hall resistance" [10]. The device characterization applied at PTB comprises four key steps:

- (1) Overview sweeps: measuring the longitudinal resistance and the Hall resistance during continuous magnetic field sweeps using the Keithley current source and nano-voltmeter.
- (2) Contact resistance: three-terminal contact resistance measurement in the QHR plateau at fixed magnetic flux density using the current source and nano-voltmeter. The suitable magnetic flux density was identified in the overview sweeps in step 1 where the longitudinal resistance drops below 1 Ω . The three-terminal resistances of all pins were below 2 Ω . Since the three-terminal resistance includes a known cable resistance of $\approx 1\Omega$ as well as the remaining longitudinal resistance of < 1 ohm, the contact resistances are estimated to be < 1 Ω .
- (3) High-accuracy characterization of ρ_{xx} and the QHR plateau: To identify the optimal operating conditions of the QHR device, the longitudinal resistance R_{xx} is determined at different B-field values. The longitudinal resistance is evaluated from the difference of two Hall resistance values determined at diagonally and orthogonally aligned contact pairs and is then converted into the geometry independent longitudinal resistivity $\rho_{xx} = w/l \times R_{xx}$ where w is the width of the Hall-channel and l the distance between the selected potential contacts along the Hall-channel. The individual Hall resistances are determined using the CCC measurement bridge and a $100~\Omega$ reference resistor. The longitudinal resistivity was identified as sufficiently low since ρ_{xx} reached a value on the order of $10~\mu\Omega$ within its combined expanded measurement uncertainty (k=2). From the measurements in step (3) the following longitudinal resistivities and s-parameter values were extracted:

The longitudinal resistivity of the GaAs-based device P876-21 along the low-potential side of the Hall bar was evaluated to be ρ_{xx} = (6.26 ± 4.65) $\mu\Omega$ at B = -9.9 T, T \approx 2.2 K, I = 38.749 μ A. The s-parameter is determined from the linear relationship s = $(R_{xy} - R_K/2)/\rho_{xx}$ between the deviation of the Hall resistance

from $R_{\rm K}/2$ and the corresponding longitudinal resistivities at several B-field values at the boundary and in the center of the QHR plateau. From the linear regression analysis of this data, the s-parameter was found to be $s = (-0.35 \pm 0.11) \, \Omega/\Omega$, resulting in a calculated deviation from $R_{\rm K}/2$ of $(-0.170 \pm 0.137) \, n\Omega/\Omega$, which was used as a correction in the $R_{\rm H}(2)/100 \, \Omega$ measurement for the evaluation of the $100 \, \Omega$ resistor value.

The uncertainties of all given quantities are combined standard uncertainties (k = 1).

(4) Uniformity checks at fixed field with the CCC involving all contact pairs: The integrity of the device was verified at fixed field (B = -9.9 T), by measuring the Hall resistances at all available orthogonally aligned contact pairs as well as at all combinations of diagonally aligned contact pairs using the CCC measurement bridge and a 100 Ω reference resistor. The Hall resistances measured at all three orthogonally aligned contact pairs were found to be consistent within 1 nΩ/ Ω . Additionally, the longitudinal resistivities along the high- and low-potential sides of the Hall bar were found to be on the level of 10 μ Ω within the combined expanded uncertainties. The identified reliable measurement conditions for the QHR using the GaAs-based device are B = -9.9 T, T ≈ 2.2 K, I = 38.749 μ Λ .

5.2.2. PTB results

The five interleaved PTB measurements of the $100~\Omega$ resistance standard based on $R_{\rm H}(2)$ were carried out using a cycled current of $38.749~\mu{\rm A}$ in the QHR (i.e. 5 mA in the $100~\Omega$) with a reversal rate of $20~\rm s$. Each PTB measurement consisted of a set of $96~\rm consecutive$ cycles but only the last $59~\rm were$ used to compute the measurement result. This means that each $20~\rm minute$ measurement ($59~\rm cycles$) was preceded by a warm-up time of around $12~\rm minutes$.

The raw and corrected measurement results are reported in Table 6 along with the starting time of measurement and dispersion (standard deviation of the mean). The 'corrected' measurements correspond to the raw measurements corrected for the difference in power dissipated in the $100~\Omega$ by PTB and BIPM. This difference results from the difference in the waveform of the reversal current cycles used by PTB and BIPM (see Figures 2 and 3), and from the small difference in the applied currents. The correction was estimated to $(+0.31\pm0.09)\times10^{-9}$ as detailed in section 5.2.3 below.

	(R _{PTB} /100	Dispersion	
Time	Raw measurements	Corrected measurements	/10-6
13:27	-0.155 72	-0.155 41	0.000 17
14:42	-0.155 60	-0.155 29	0.000 17
15:57	-0.155 56	-0.155 25	0.000 14
17:07	-0.155 57	-0.155 26	0.000 12
18:18	-0.155 89	-0.155 58	0.000 18
	Mean value	-0.155 36	
	Standard deviation, u_A	0.000 12	

Table 6: PTB measurements of the $100~\Omega$ standard in terms of $R_{\rm H}(2)$ using the GaAs QHR device P-876-21, on May 8, 2025. Results are expressed as the relative difference from the nominal $100~\Omega$ value. Time corresponds to the starting time of measurement and the dispersion to the standard deviation of the mean of the measurements considered.

The resistance value R_{PTB} reported below corresponds to the mean of 100 Ω measurements carried out by the PTB, corrected for the difference in power dissipated in the resistor, on May 8, 2025.

Mean value: $R_{PTB} = 100 \times (1 - 0.155 \ 36 \times 10^{-6}) \Omega$

Relative standard uncertainty: $u_{PTB} = 0.21 \times 10^{-9}$

where u_{PTB} is calculated as the root sum square of: $u_{\text{A}} = 0.12 \times 10^{-9}$ (Table 6), $u_{power} = 0.09 \times 10^{-9}$ the standard uncertainty on power correction and $u_{\text{B}} = 0.151 \times 10^{-9}$ (Table 4).

Note that the above given value of u_{PTB} would have been about 0.19×10^{-9} if no power correction were applied on the measured value of R_{PTB} .

5.2.3. Estimation of the power correction applied on the PTB 100 Ω measurements

The 100 Ω resistance standard has a non-zero power coefficient that has been previously determined at the BIPM. The differences in shape and magnitude of the reversal current cycles used by PTB and BIPM for the comparison therefore induce a difference of the effective powers dissipated in the 100 Ω resistor during the measurements.

From the magnitude and shape differences of the current cycles used by the BIPM and PTB CCC bridges, it was estimated that the effective power dissipated in the resistor by PTB is (0.35 ± 0.05) mW higher than that dissipated by BIPM. Considering the power coefficient of the $100~\Omega$ standard, estimated as (-0.87 ± 0.34) parts in 10^9 per mW, a power correction was computed and applied to the PTB measurement results. This correction was estimated as (0.31 ± 0.09) parts in 10^9 .

5.3. 100Ω measurements comparison

Figure 4 presents the corrected interleaved measurements from PTB and BIPM on May 8, 2025. Error bars correspond to the dispersion observed for each measurement.

No significant instabilities of the 100 Ω transfer resistor were observed within the limit of the dispersion of the results and therefore no additional uncertainty component was included in the final comparison results.

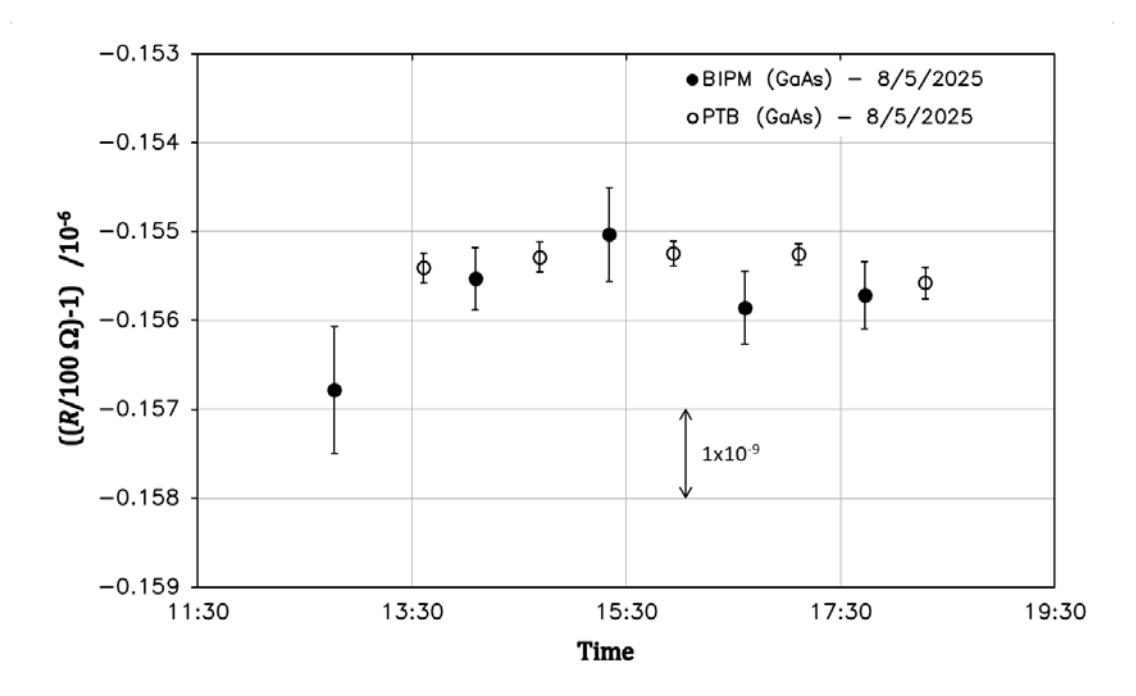


Figure 4: PTB (open circles) and BIPM (black dots) corrected measurements of the 100 Ω resistance $R_{100\Omega}$ in terms of $R_{\rm H}(2)$ on May 8, 2025. The error bars correspond to the dispersion observed for each measurement.

The difference between PTB and BIPM was then calculated as the difference between the corrected means of the series of measurements carried out by both institutes on May 8, 2025 (from Tables 5 and 6):

Relative difference PTB-BIPM: $(R_{PTB} - R_{BIPM}) / R_{BIPM} = 0.4 \times 10^{-9}$

with a relative combined standard uncertainty: $u_{\text{comp}} = 2.1 \times 10^{-9}$

where u_{comp} is calculated as the root sum square of $u_{\text{BIPM}} = 2.1 \times 10^{-9}$ and $u_{\text{PTB}} = 0.21 \times 10^{-9}$.

6. Measurement of the 100 Ω transfer standard in terms of $R_{\rm H}(2)$ using GaAs- and graphene-based QHE devices

The comparison of the $100\,\Omega$ transfer standard measurements was repeated in the exact same conditions as in the previous section 5, except that PTB used a graphene-based QHR standard fabricated in PTB's clean room facility instead of a GaAs-based one. BIPM kept the same GaAs-based QHR standard.

As mentioned earlier, this is the first time in this comparison program that these two different types of QHR references are used for the realization of the ohm at $100\,\Omega$. The continuous improvement of the fabrication techniques of graphene-based QHR devices over the past decade now makes it possible to produce such references with metrological performances identical to those based on GaAs, but at significantly relaxed operating conditions: temperature of 4.2 K, magnetic flux density of 5 T or less, and higher current amplitude of several $100~\mu A$ [17-21]. Thus, several NMIs have started to use graphene-based devices for the realization of the ohm as a primary standard or are about to do so.

The question of the long-term stability of these references, which depends quite strongly on storage conditions, remains unresolved for the moment, as it was for GaAs-based QHRs when they first appeared. Nevertheless, several studies have already demonstrated their stability over several years [17, 22].

At the time of this comparison, a working group of the CCEM is drafting an addendum to the current guidelines for the implementation of GaAs-based QHRS [10] to specify the preliminary checks required for reliable use of graphene-based QHRS for precision measurements. Pending the forthcoming publication of this document, the guidelines for GaAs-based QHRS have been used for the characterization of the graphene-based QHRS used by PTB. Some additional specific checks were also carried out (sheet resistances, carrier density, mobility, determination of minimum operating flux density) that are described, for instance, in reference [23].

6.1. BIPM measurements

As mentioned above, the GaAs-based QHRS used by the BIPM for these measurements is the same as for the measurements described in section 5.

6.1.1. Preliminary tests

The QHR was operated in the same condition, on the i=2 plateau at a temperature of 1.4 K, a flux density of about 10.5 T and with a rms current of 40 μ A.

The QHR device was tested again as explained in Section 5.1.1. In particular, the absence of significant longitudinal dissipation on either side of the device was verified and found to be less than 5×10^{-10} in relative terms with a standard deviation of the same order. The uncertainty component for the imperfect realization of the QHR (Table 2) considers a possible error due to the longitudinal dissipation. The uniformity of the measurements between the three opposite orthogonal contact pairs was found to be of the order of 3×10^{-10} . The series of measurements performed subsequently for the purpose of the comparison were taken from the central pair of contacts only.

The two terminal Hall resistance of the four terminal pairs device was measured and showed that the contact resistance was smaller than a few ohms (measurements limited by the resolution of the handheld multimeter used). This measurement was repeated before and after each series of comparison measurements.

6.1.2. BIPM results

On May 13, 2025, a series of six BIPM measurements of the 100 Ω standard based on $R_{\rm H}(2)$ were interleaved with six PTB measurements. The same 100 Ω (Tegam s/n: A 2030405SR102) was used and the measurements were conducted in the exact same conditions as described in section 5.1.2.

The measurements of the 100 Ω standard carried out at 1 Hz by the BIPM are reported in Table 7 as well as the 'dc' corrected values (using the 1 Hz-'dc' correction from Table 1). Both are expressed as the relative difference from the 100 Ω nominal value: ($R_{\rm BIPM}/100~\Omega$) - 1. Each of the measurements reported in the table is the average value of a series of five individual measurements and corresponds to a total measurement time of about 19 minutes.

	$(R_{\rm BIPM}/100 \Omega)$ -1 /10 ⁻⁶		
Time	1 Hz measurements	ʻdc' corrected (with 1 Hz-ʻdc' correction)	Dispersion /10 ⁻⁶
12:54	-0.159 70	-0.153 70	0.000 32
14:19	-0.159 37	-0.153 37	0.000 26
15:34	-0.161 60	-0.155 60	0.000 30
16:46	-0.160 42	-0.154 42	0.000 46
17:57	-0.160 66	-0.154 66	0.000 50
19:30	-0.161 27	-0.155 27	0.000 92
	Mean value	-0.154 50	
	Standard deviation, u_A	0.000 79	

Table 7: BIPM measurements of the $100~\Omega$ standard in terms of $R_{\rm H}(2)$ on May 13, 2025. Results are expressed as the relative difference from the nominal $100~\Omega$ value. Each measurement is the average value of a series of five individual measurements. Time corresponds to the starting time of this measurement series and the dispersion to the standard deviation of the mean.

The resistance value R_{BIPM} reported below corresponds to the mean of the corrected measurements carried out by the BIPM on May 13, 2025:

Mean value: $R_{\text{BIPM}} = 100 \times (1 - 0.1545 \times 10^{-6}) \Omega$

Relative standard uncertainty: $u_{BIPM} = 2.2 \times 10^{-9}$

where u_{BIPM} is calculated as the root sum square of $u_A = 0.8 \times 10^{-9}$ (Table 7) and $u_B = 2.0 \times 10^{-9}$ (Table 2).

6.2. PTB measurements

In this repetition of the 100 Ω comparison measurements based on $R_{\rm H}(2)$, PTB used a graphene-based quantum Hall resistance standard.

6.2.1. Preliminary tests

The probe with the mounted graphene device G1534_F13#6 is cooled from room temperature to 4.2 K with all contacts short-circuited to each other and to the probe housing. After the cooldown is completed, the short-circuit is removed. To start with the characterization, the probe is connected through an eight-

pin interface to a PC-controlled measurement setup comprising a precision current source, and a nanovoltmeter (Keithley 6220 and 2182, respectively).

The characterization procedure of the QHR device follows the methods described in the established "Revised technical guidelines for reliable dc measurements of the quantized Hall resistance" [10]. The device characterization applied at PTB comprises four key steps:

- (1) Overview sweeps: measuring the longitudinal resistance and the Hall resistance during continuous magnetic field sweeps using the Keithley current source and nano-voltmeter.
- (2) Contact resistance: three-terminal contact resistance measurement in the QHR plateau at fixed magnetic flux density using the Keithley current source and nano-voltmeter. The suitable magnetic flux density was identified in the overview sweeps in step 1 where the longitudinal resistance drops below 1 Ω . The three-terminal resistances of all pins were below 2 Ω . Since the three-terminal resistance includes a known cable resistance of $\approx 1\Omega$ as well as the remaining longitudinal resistance of <1 ohm, the contact resistances are estimated to be <1 Ω .
- (3) High-accuracy characterization of ρ_{xx} and the QHR plateau: To identify the optimal operating conditions of the QHR device, the longitudinal resistance R_{xx} is determined at different B-field values. The longitudinal resistance is evaluated from the difference of two Hall resistance values determined at diagonally and orthogonally aligned contact pairs and is then converted into the geometry independent longitudinal resistivity $\rho_{xx} = w/l \times R_{xx}$ where w is the width of the Hall-channel and l the distance between the selected potential contacts along the Hall-channel. The individual Hall resistance values are determined using the CCC measurement bridge and a $100~\Omega$ reference resistor. The longitudinal resistivity was identified as sufficiently low since ρ_{xx} reached a value on the order of $10~\mu\Omega$ within its combined expanded measurement uncertainty (k=2). From the measurements in step (3) the following longitudinal resistivities and s-parameter values were extracted:

The longitudinal resistivity of the graphene-based device G1534_F13#6 was found to be ρ_{xx} = (14.35 ± 4.06) $\mu\Omega$ along the low-potential side of the Hall device at B = -5.0 T, T = 4.2 K, I = 38.749 μ A. The s-parameter is determined from the linear relationship s = (R_{xy} - $R_{K}/2$)/ ρ_{xx} between the deviation of the Hall resistance from $R_{K}/2$ and the corresponding longitudinal resistivities at several B-field values at the boundary of and inside the QHR plateau. From the linear regression analysis of this data, the s-parameter was identified to be s = (-0.219 ± 0.008) Ω/Ω , resulting in a calculated deviation from $R_{K}/2$ of (-0.244 ± 0.070) $n\Omega/\Omega$ which was then used as a correction in the $R_{H}(2)/100$ Ω measurement for the evaluation of the 100 Ω resistor value.

The uncertainties of all given quantities are combined standard uncertainties (k = 1).

(4) Uniformity check at fixed field with the CCC involving all contact pairs: The integrity of the device was verified at fixed field (B = -5.0 T), by measuring the Hall resistances at all available orthogonally aligned contact pairs as well as at all combinations of diagonally aligned contact pairs using the CCC measurement bridge and a 100 Ω reference resistor. The Hall resistances measured at all three orthogonally aligned contact pairs were found to be consistent within $1 \text{ n}\Omega/\Omega$. Additionally, the longitudinal resistivities along the high- and low-potential sides of the Hall bar in both devices were found to be on the order of $10 \text{ }\mu\Omega$. The identified reliable measurement conditions for the QHR using the graphene-based device were B = -5.0 T, T = 4.2 K, I = 38.749 μ A.

6.2.2. PTB results

The six interleaved PTB measurements of the $100~\Omega$ resistance standard based on $R_H(2)$ were performed using a cycled current of $38.749~\mu A$ in the QHR (i.e. 5~mA in the $100~\Omega$) with a reversal rate of 20~s. Similarly to measurements made using the GaAs-based QHR device (section 5.2.2), each PTB measurement consisted of a set of 96 consecutive cycles but only the last 59 were used to compute the measurement result (20-minute measurement preceded by a warm-up time of around 12~minutes).

The raw and corrected measurement results are presented in Table 8, along with the average measurement time and dispersion (standard deviation of the mean). The 'corrected' measurements correspond to the raw measurements corrected for the difference in powers dissipated in the $100\,\Omega$ by PTB and BIPM. This difference results from the difference in the waveform of the reversal current cycles used by PTB and BIPM (see Figures 2 and 3), and from the small difference in the magnitude of the applied currents. The correction was estimated to $(0.31\pm0.09)\times10^{-9}$ as previously detailed in section 5.2.3.

	$(R_{\rm PTB}/100~\Omega)$ -1 /10 ⁻⁶		Dispersion
Time	Raw measurements	Corrected measurements	/10 ⁻⁶
13:39	-0.154 84	-0.154 53	0.000 18
14:52	-0.155 05	-0.154 74	0.000 17
16:04	-0.154 98	-0.154 67	0.000 19
17:16	-0.154 98	-0.154 67	0.000 22
18:37	-0.154 46	-0.154 15	0.000 24
20:06	-0.154 64	-0.154 33	0.000 16
	Mean value	-0.154 52	
	Standard deviation, u_A	0.000 21	

Table 8: PTB measurements of the $100~\Omega$ standard in terms of $R_{\rm H}(2)$ using the graphene QHR device G1534_F13#6, on May 13, 2025. Results are expressed as the relative difference from the nominal $100~\Omega$ value. Time corresponds to the starting time of measurement and the dispersion to the standard deviation of the mean of the measurements considered.

The resistance value R_{PTB} reported below corresponds to the mean of 100 Ω measurements carried out by the PTB, corrected for the difference in powers dissipated in the resistor, on May 13, 2025.

Mean value: $R_{PTB} = 100 \times (1 - 0.154 \ 52 \times 10^{-6}) \Omega$

Relative standard uncertainty: $u_{\text{PTB}} = 0.25 \times 10^{-9}$

where u_{PTB} is calculated as the root sum square of: $u_{\text{A}} = 0.21 \times 10^{-9}$ (Table 8), $u_{power} = 0.09 \times 10^{-9}$ the standard uncertainty on power correction and $u_{\text{B}} = 0.094 \times 10^{-9}$ (Table 4).

Note that the above given value of u_{PTB} would have been about 0.23×10^{-9} if no power correction were applied on the measured value of R_{PTB} .

6.3. 100Ω measurements comparison

Figure 5 presents the corrected interleaved measurements from PTB and BIPM on May 13, 2025. Error bars correspond to the dispersion observed for each measurement.

Although the BIPM measurement results appear less stable than those of the PTB, all measurements are still fully comparable within the limits of the measurement uncertainties (2×10^{-9}) for BIPM. The observed instabilities are believed to be due to stability issues of the 1 Hz bridge during this series of measurements. No clear explanation for these instabilities was found in the course of the measurements although it is believed that they are related to intermittent disturbances on the ground path chosen for the BIPM measuring system. More time would have been needed to investigate another grounding configuration.

No specific instability or drift can be attributed to the $100\,\Omega$ transfer resistor and therefore no associated uncertainty component was included in the final comparison results.

The difference between PTB and BIPM was then calculated as the difference between the corrected means of the series of measurements carried out by both institutes on May 13, 2025 (from Tables 7 and 8):

Relative difference PTB-BIPM: $(R_{\text{PTB}} - R_{\text{BIPM}}) / R_{\text{BIPM}} = 0.0 \times 10^{-9}$

with a relative combined standard uncertainty: $u_{\text{comp}} = 2.2 \times 10^{-9}$

where u_{comp} is calculated as the root sum square of $u_{\text{BIPM}} = 2.2 \times 10^{-9}$ and $u_{\text{PTB}} = 0.25 \times 10^{-9}$.

Considering the comparison uncertainty, the above relative PTB-BIPM difference for the measurement of the 100 Ω value based on $R_{\rm H}(2)$ is consistent to that obtained previously where both, BIPM and PTB used a GaAs-based QHRS (section 5.3).

As already shown in several previous informal interlaboratory comparisons, this result proves once again that graphene-based QHE devices offer similar performances as GaAs-based ones, with the advantage that they can be used under relaxed conditions (B=-5 T and T=4.2 K in the present comparison).

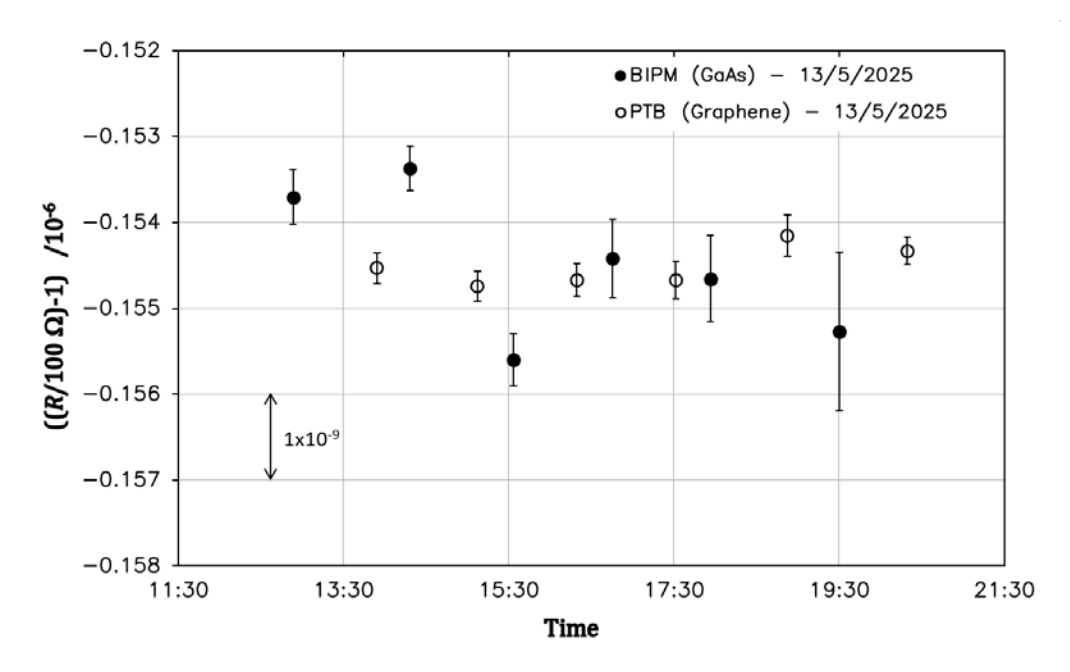


Figure 5: PTB (open circles) and BIPM (black dots) corrected measurements of the 100 Ω resistance $R_{100\Omega}$ in terms of $R_{\rm H}(2)$ on May 13, 2025. The error bars correspond to the dispersion observed for each measurement.

7. Additional comparison measurement of the GaAs- and graphene-based QHE devices

An additional direct comparison measurement of the GaAs- and graphene-based QHE devices used in sections 6 was carried out on May 14, 2025 at 12:23pm. In this measurement, the two devices were compared in a 1:1 ratio using PTB's CCC bridge, thus avoiding the use of the $100~\Omega$ transfer standard.

For this measurement, full current reversal cycles with a duration of 20 s and a current magnitude of $38.749~\mu A$ were applied to the two QHE devices. A total of 120 measurement cycles were applied and the difference between the two QHR devices was computed using the last 91 cycles (i.e. 30 minutes of measurement).

The measured difference between the PTB graphene-based QHR and the GaAs-based BIPM QHR was:

Relative difference PTB-BIPM: $(R_{\text{graphene_PTB}} - R_{\text{GaAs_BIPM}}) / R_{\text{GaAs_BIPM}} = -0.5 \times 10^{-9}$

with a relative combined standard uncertainty: $u_{\text{comp}} = 0.8 \times 10^{-9}$

where u_{comp} is calculated as the root sum square of $u_{\text{BIPM}} = 0.8 \times 10^{-9}$ due to the imperfect quantization of the BIPM QHR (from Table 2) and $u_{\text{QHRs_ratio}} = 0.21 \times 10^{-9}$, corresponding to the combined measurement uncertainty of the QHRs ratio with the PTB CCC bridge (from Table 4). Note that a correction of -0.24×10^{-9} was applied to compensate for the imperfect quantization of the PTB graphene-based QHR.

It should be noted that, although this direct comparison was performed over a limited measurement period, it yielded very convincing results, demonstrating the equivalence of the two types of QHRS within about $1\,\mathrm{n}\Omega/\Omega$ and thereby further supporting the results reported in Section 6.

8. Measurement of K1 ratio (10 k Ω /100 Ω)

8.1. BIPM measurements of K1

For the measurement of K1 ratio the 129:1 LFCC equipping the BIPM 1 Hz bridge for the $R_{\rm H}(2)/100\,\Omega$ ratio measurement was replaced by a 100:1 LFCC. The 100 Ω and 10 k Ω standards referenced s/n: A 2030405SR102 and s/n: K 201119630104, respectively, were used. The rms current in the 10 k Ω standard was 50 μ A corresponding to 5.0 mA in the 100 Ω standard.

On May 9, 2025, the 10 $k\Omega$ and 100 Ω standards were connected alternately to the BIPM and PTB bridges and five BIPM measurements were interleaved with five PTB measurements. After each bridge change, at least 10 minutes were allowed for thermal stabilization of the connections, with measurement current applied.

The raw and corrected BIPM measurements are reported in Table 9 (relative difference from nominal ratio 100). Each of the raw measurements is the mean value of seven individual measurements corresponding to a total measurement time of about 26 minutes. The corrected measurements correspond to the raw data to which the 1 Hz - dc correction reported in Table 1 was applied. The associated dispersion is estimated by the standard deviation of the mean of the seven individual measurements.

	(K1 _{BIPM} /100)-1 /10 ⁻⁶		Dispersion	
Time	1 Hz measurements	'dc' corrected (with 1 Hz-'dc' correction)	/10 ⁻⁶	
10:02	1.648 34	1.649 31	0.000 67	
12:42	1.648 00	1.648 96	0.000 54	
14:15	1.646 93	1.647 90	0.000 46	
15:45	1.646 72	1.647 69	0.000 77	
18:19	1.645 93	1.646 90	0.000 57	
	Mean value	1.648 15		
	Standard deviation, u_A	0.000 88		

Table 9: BIPM measurements of the ratio K1 on May 9, 2025. Results are expressed as the relative difference from the nominal ratio value 100. Each measurement is the mean value of a series of seven individual measurements. Time corresponds to the starting time of this measurement series and the dispersion to the standard deviation of the mean.

The *K*1 ratio value reported below corresponds to the mean of the corrected ratio measurements carried out by the BIPM on May 9, 2025.

Mean value: $K1_{BIPM} = 100 \times (1 + 1.6482 \times 10^{-6})$

Relative standard uncertainty: $u_{\text{BIPM}} = 2.0 \times 10^{-9}$

where u_{BIPM} is calculated as the root sum square of u_{A} = 0.9 × 10⁻⁹ (Table 9) and u_{B} = 1.8 × 10⁻⁹ (Table 2).

8.2. PTB measurements of K1

For K1 ratio measurements, the currents through the $100\,\Omega$ and $10\,k\Omega$ resistance standards were 5 mA and $50\,\mu$ A, respectively. A current reversal cycle time of $20\,s$ was used.

As with the $R_{100\Omega}$ measurement, a correction was made to account for the difference in dissipated powers between BIPM and PTB in the $100~\Omega$ and $10~k\Omega$ standards. This correction was estimated from the power coefficient of the ratio K1 and from the effective difference of power dissipated in the resistors between the PTB and the BIPM. The latter was computed from the current magnitudes and cycle timing parameters used by each of the institutes and considering that the power was only dissipated in the $100~\Omega$ standard (negligible dissipation in the $10~k\Omega$ standard). It was estimated that the power dissipated by PTB in the $100~\Omega$ was (0.47 ± 0.03) mW higher than that dissipated by BIPM. Thus, using the power coefficient $(1.35 \pm 0.43) \times 10^{-9}$ per mW of the ratio K1 – determined by the BIPM prior to the comparison – the power difference correction of the K1 ratio was in turn estimated to be $(-0.63 \pm 0.14) \times 10^{-9}$.

As mentioned earlier, five PTB measurements were interleaved with five BIPM measurements. Each PTB measurement consisted of a set of 111 consecutive full cycles but only the last 75 were used to compute the measurement result (25-minute measurement preceded by a warm-up time of around 12 minutes).

The raw and corrected measurement results of PTB are reported in Table 10. They are expressed as the relative difference from the nominal ratio value 100 with a dispersion corresponding to the standard deviation of the mean of the individual measurements.

	Standard deviation, u_A	0.000 54	
	Mean value	1.647 47	
19:04	1.647 82	1.647 19	0.000 68
16:26	1.647 72	1.647 09	0.000 66
14:59	1.648 91	1.648 28	0.000 72
13:28	1.64749	1.646 86	0.000 65
11:45	1.648 54	1.647 91	0.000 69
Time	Raw measurements	'power' corrected measurements	Dispersion /10 ⁻⁶
(K1 _{PTB} /100)		0)-1 /10-6	Dignorgion

Table 10: PTB measurements of the ratio *K*1 on May 9, 2025. Results are expressed as the relative difference from the nominal ratio value 100. Time corresponds to the starting time of measurement and the dispersion to the standard deviation of the mean of each individual measurement.

The *K*1 ratio value reported below corresponds to the mean of the ratio measurements carried out by the PTB on May 9, 2025.

Mean value: $K1_{PTB} = 100 \times (1 + 1.647 \, 47 \times 10^{-6})$

Relative standard uncertainty: $u_{PTB} = 0.56 \times 10^{-9}$

where u_{PTB} is calculated as the root sum square of: $u_{\text{A}} = 0.54 \times 10^{-9}$ (Table 10), $u_{power} = 0.14 \times 10^{-9}$ the standard uncertainty on power difference correction and $u_{\text{B}} = 0.06 \times 10^{-9}$ (Table 4).

Note that the above given value of u_{PTB} would have been about 0.54×10^{-9} if no power correction were applied on the measured value of $K1_{PTB}$.

8.3. Comparison of K1 measurements

Figure 6 presents the interleaved corrected measurements from PTB and BIPM on May 9, 2025. Error bars correspond to the dispersion observed for each measurement.

No clear drift or significant instability was detected in the *K*1 measurements within the limit of the comparison uncertainty and therefore no specific additional uncertainty component was included in the final comparison results.

The relative difference between PTB and BIPM was calculated from the difference of the means of the measurement series carried out by both institutes on May 9, 2025 (from Tables 9 and 10):

Relative difference PTB-BIPM: $(K1_{PTB} - K1_{BIPM}) / K1_{BIPM} = -0.7 \times 10^{-9}$

with a relative combined standard uncertainty: $u_{\text{comp}} = 2.1 \times 10^{-9}$

where u_{comp} is calculated as the root sum square of $u_{\text{BIPM}} = 2.0 \times 10^{-9}$ and $u_{\text{PTB}} = 0.56 \times 10^{-9}$.

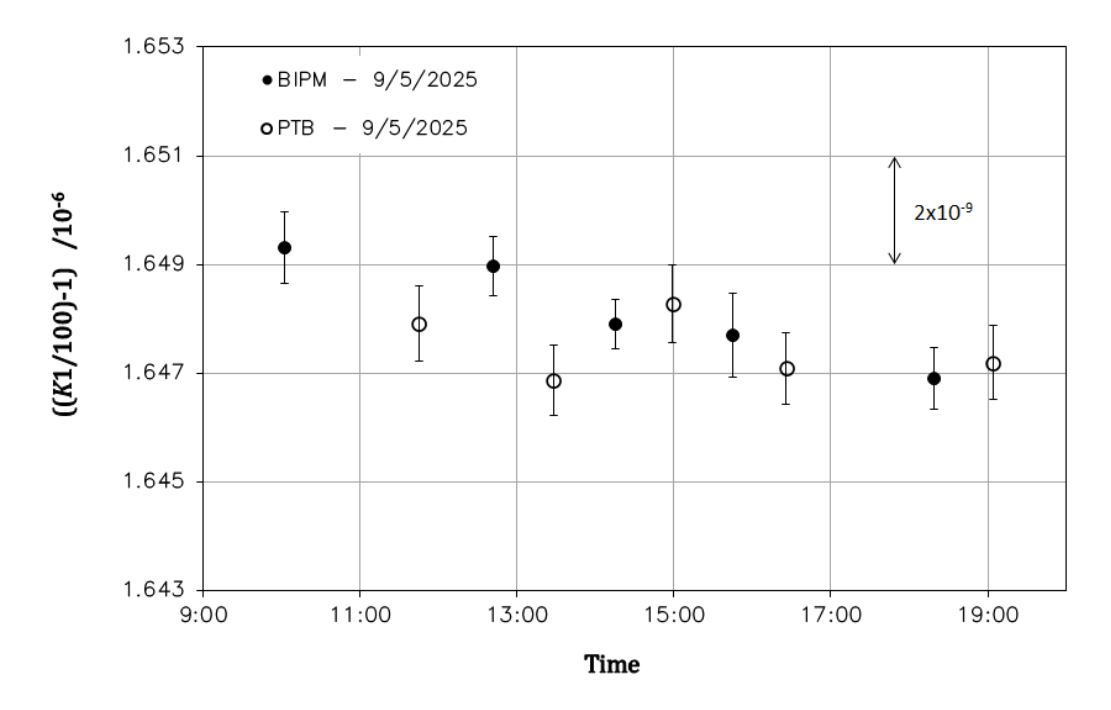


Figure 6: PTB (open circles) and BIPM (black dots) corrected measurements of the ratio *K*1 on May 9, 2025. The error bars correspond to the dispersion observed during each measurement.

9. Measurement of K2 ratio (100 $\Omega/1 \Omega$)

9.1. Preliminary measurements: influence of the current reversal cycle time

Previous studies [3-8] have shown that close attention must be paid to the influence of the Peltier effect in the $1\,\Omega$ standard when measuring the K2 ratio. In particular, it has been shown in [3,5,6] that the Peltier effect induces a decrease in the K2 value as the current reversal cycle time increases (at least up to the usual BIPM CCC cycle time of about 340 s), preventing the true "dc" value of this ratio from being reached. However, it was also observed that it exists a threshold cycle time (typically of the order of 10 s to a few tens of seconds) below which K2 measurements remain stable within the usual best measurement uncertainties as those that can be reached in the present comparison.

This is why, in previous BIPM.EM-K12 comparisons since 2013, the *K*2 measurements were carried out using short cycle times, for which the error due to Peltier effect – and possibly cable influence – is limited or null. Preliminary measurements are therefore necessary to determine the threshold value of the reversal cycle time below which the *K*2 ratio remains stable. Below this threshold value, the measurement made by the participating NMI can be directly compared with the BIPM measurement performed with its 1 Hz bridge (1 s period sinusoidal reversal cycle).

In the present comparison, we used for the first time a new type of 1 Ω standard resistor (model HRU-1R0 manufactured by Alpha Electronics on the basis of an AIST-NMIJ design) which is expected to have reduced cycle time dependence. This assertion is based on an in-depth study of the influence of cycle time on this type of resistance – carried out in collaboration with the PTB and the NMIJ – which is summarised in [24]. This study also highlighted a possible influence of the measuring cable used on the dependence of the K2 value on the reversal cycle time.

Preliminary measurements to verify the possible dependence of K2 (i.e. of the 1 Ω HRU-1R0 resistance standard) on cycle time were carried out using PTB's CCC bridge. The cycle time was varied from 6 s to 340 s in the sequence of 10 s, 20 s, 40 s, 6 s, 10 s and 340 s. The timing details of the cycles are reported in Table 3. The measurement with a cycle time of 340 s was taken over several hours during the night. For these measurements, the current magnitude in the 100 Ω and 1 Ω standards were 0.5 mA and 50 mA, respectively. All the other experimental conditions were the same as those used for the measurement of K1 ratio. Care was taken that PTB and BIPM use similar measuring cables.

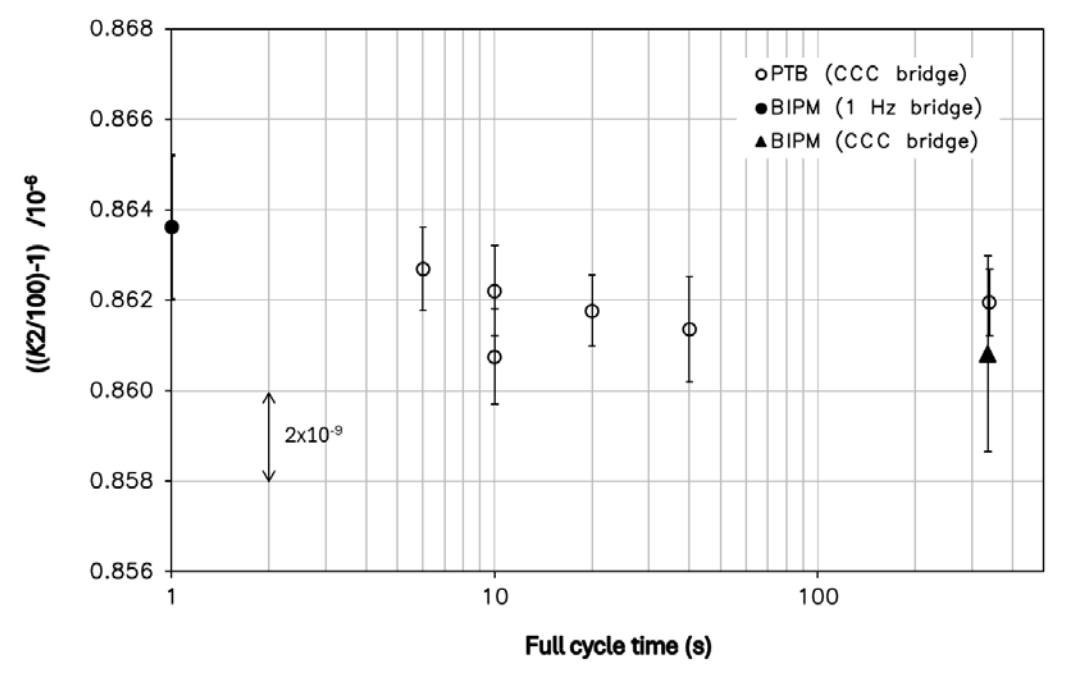


Figure 7: Preliminary measurements of the *K*2 ratio performed by PTB when the current reversal cycle time is varied from 6 s to 340 s (open circles). For comparison, a measurement at 1 Hz made by BIPM is added to the graph (full circle). The data point indicated by the triangle shows the calculated eqivalent dc value of BIPM's CCC bridge, which corresponds to the 1 Hz measurement corrected by the 1 Hz-dc difference of *K*2 ratio and by the power difference resulting from the difference in shape of BIPM's and PTB's CCC reversal cycles.

Figure 7 shows the results of the preliminary *K*2 ratio measurements made by PTB with its CCC bridge. For the sake of comparison, a 1 Hz measurement was carried out by BIPM with the 1 Hz bridge just after PTB completed the series of measurements with different cycle times of 10 s, 20 s, 40 s, 6 s, 10 s. BIPM's 1 Hz result corresponds to the black dot symbol while the calculated equivalent BIPM CCC value is

represented by the triangle. The latter equivalent measurement value is obtained by correcting the 1 Hz measurement for the 1 Hz-dc difference from Table 1 and for the power difference in the 1 Ω resistor associated with the difference in shape of the CCC bridge reversal cycles of the BIPM and PTB (see figures 2 and 3). The error bars correspond to combined uncertainties of the measurements. The two measurements for the 10 s cycle time give an idea of the reproducibility of the measurements (measurements at the start and end of the sequence, 80 minutes apart).

It can be seen from Figure 7 that the value of the K2 ratio is independent of the cycle time within the measurement uncertainties. All measurements do not differ by more than 3×10^{-9} between 1 s and 340 s which verifies the conclusion of [24] for this type of 1 Ω resistor.

Therefore, the comparison of the *K*2 ratio could be carried out in the same way as for *K*1, i.e. by comparing the results for cycle times of 20 s and 336 s for the PTB and BIPM CCC bridges, respectively. However, to remain consistent with the previous comparisons, it has been decided to continue to compare the BIPM 1 Hz measurement with a short cycle PTB measurement. A full cycle duration of 10 s was chosen by PTB.

9.2. Influence of comparing measurements at 1 Hz on the BIPM uncertainty budget

When the 1 Hz bridge of the BIPM is no longer used as a transfer instrument referenced to its CCC bridge, one has to consider the uncertainty associated with the accuracy of its room temperature current comparator and resistive divider [11]. The uncertainty budget for the use of the BIPM 1 Hz bridge for the measurement of the ratio K2 is reported in Table 11.

Furthermore, although no clear influence of the Peltier effect is observed in measurements between cycle times of 1 s and 10 s (figure 7), its influence is still considered as possible within the limit of $\pm 1 \times 10^{-9}$. A relative standard uncertainty of $u_{\text{Peltier}} = 1 \times 10^{-9}$ will therefore be taken into account in the calculation of the comparison uncertainty.

Resistance ratio $K2 (100 \Omega/1 \Omega)$		
Relative standard uncertainties	/10-9	
Ratio error of the room temperature current comparator	1.5	
Resistive divider calibration of the secondary current source	0.5	
Finite gain of servo of the bridge balance	0.5	
Combined type B standard uncertainty, $u_{\rm B}$	1.7	

Table 11: Uncertainty budget for the measurement at 1 Hz of the *K*2 ratio using the BIPM 1 Hz bridge (the 1 Hz bridge being no longer used as a transfer instrument referenced to the BIPM CCC bridge).

9.3. BIPM measurements of K2

For the measurement of K2, two resistance standards from Alpha Electronics were used. The 100 Ω was of type HRU-101 (s/n: F078) and the 1 Ω of type HRU-1R0 (s/n: F112A). The rms current in the 100 Ω standard was 0.5 mA corresponding to 50 mA in the 1 Ω standard.

On May 12, 2025, the 100 Ω and 1 Ω standards were connected alternately to the BIPM and PTB bridges and five BIPM measurements at 1 Hz were interleaved with five PTB measurements. After each bridge change, at least 5 minutes were allowed for the thermal stabilization of the connections, with measurement current applied.

The BIPM measurements at 1 Hz, expressed as the relative difference with respect to the nominal ratio of 100, are shown in Table 12. Each of the raw measurements is the mean value of six individual measurements corresponding to a total measurement time of about 22 minutes. The associated dispersion is estimated by the standard deviation of the mean of the six individual measurements.

Time	(К2вірм/100)-1 /10-6	Dispersion
	1 Hz measurements	/10-6
12:52	0.863 62	0.000 54
14:22	0.863 12	0.000 84
15:29	0.865 05	0.000 60
16:39	0.865 71	0.000 43
17:47	0.865 14	0.000 67
Mean value	0.864 53	
Standard deviation, u_A	0.000 99	

Table 12: BIPM measurements of the ratio *K*2 carried out on May 12, 2025. Results are expressed as the relative difference from the nominal ratio value 100. Each measurement is the mean value of a series of six individual measurements. Time corresponds to the starting time of this measurement series and the dispersion of the standard deviation of the mean.

The *K*2 ratio value reported below corresponds to the mean of the 1 Hz ratio measurements carried out by the BIPM on May 12, 2025.

Mean value: $K2_{BIPM} = 100 \times (1 + 0.8645 \times 10^{-6})$

Relative standard uncertainty: $u_{\text{BIPM}} = 2.0 \times 10^{-9}$

where $u_{\rm BIPM}$ is calculated as the root sum square of $u_{\rm A}$ =1.0 × 10⁻⁹ (Table 12) and $u_{\rm B}$ = 1.7 × 10⁻⁹ (Table 11)

9.4. PTB measurements of K2

For $\mathit{K2}$ ratio measurements, the currents through the 100 Ω and 1 Ω resistance standards were 0.5 mA and 50 mA, respectively. For the reason explained in section 9.1, a current reversal cycle time of 10 s was used by PTB.

Five PTB measurements were interleaved with five BIPM measurements. Each PTB measurement consisted of a set of 149 consecutive cycles but only the last 119 were used to compute the measurement result (20-minute measurement preceded by a warm-up time of around 5 minutes).

As with the $R_{100\Omega}$ and K1 measurement, a correction was applied to account for the differences in power dissipation in the two resistors (100 Ω and 1 Ω standards) due to the different bridge current excitations used by BIPM and PTB. This correction was estimated from the power coefficient of the ratio K2 and from the effective difference of power dissipated in the resistors between the PTB and the BIPM. The latter was computed from the current magnitudes and cycle timing parameters used by each of the institutes and assuming that the power was only dissipated in the 1 Ω standard (negligible dissipation in the 100 Ω standard).

It was estimated that the power dissipated by PTB in the $1\,\Omega$ was (0.08 ± 0.05) mW lower than that dissipated by BIPM. Thus, using the power coefficient $(2.68 \pm 0.48) \times 10^{-9}$ per mW of the ratio K2 – determined by the BIPM prior to the comparison – the power difference correction to be applied to the K2 ratio was in turn estimated to be $(0.21 \pm 0.10) \times 10^{-9}$.

The raw measurement results of PTB as well as those corrected for difference in power dissipation are reported in Table 13. They are expressed as the relative difference from the nominal ratio value 100 with a dispersion corresponding to the standard deviation of the mean of the individual measurements.

m:	(K2 _{PTB} /100)-1 /10 ⁻⁶		Dispersion
Time	Raw measurements	Corrected measurements	/10-6
13:40	0.862 98	0.863 19	0.000 74
14:55	0.862 29	0.862 50	0.000 91
16:03	0.864 93	0.865 14	0.000 82
17:13	0.864 19	0.864 40	0.000 85
18:33	0.863 98	0.864 19	0.000 80
Mean value		0.863 88	
Standard deviation, u_A		0.000 93	

Table 13: PTB measurements of the ratio *K*2 carried out on May 12, 2025. Results are expressed as the relative difference from the nominal ratio value 100. Time corresponds to the starting time of measurement and the dispersion to the standard deviation of the mean of each individual measurement.

The *K*2 ratio value reported below corresponds to the mean of the corrected ratio measurements carried out by the PTB on May 12, 2025.

Mean value: $K2_{PTB} = 100 \times (1 + 0.863 88 \times 10^{-6})$

Relative standard uncertainty: $u_{PTB} = 0.94 \times 10^{-9}$

where u_{PTB} is calculated as the root sum square of $u_A = 0.93 \times 10^{-9}$ (Table 13), $u_{power} = 0.10 \times 10^{-9}$ the standard uncertainty on power difference correction and $u_B = 0.06 \times 10^{-9}$ (Table 4).

9.5. Comparison of K2 measurements

The interleaved measurements of the BIPM and PTB, carried out at 1 Hz and for a full cycle time of 10 s respectively, are reported in Figure 8.

The error bars in Figure 8 correspond to the dispersion observed for each of the measurements. It can be seen that a small jump of K2 value of about 2 $n\Omega/\Omega$ occurred after the first two BIPM and PTB measurements. This jump was detected by the BIPM and PTB measurement systems and is most likely due to a jump in the value of one of the resistance standards (increase of the 100Ω or decrease of the 1Ω).

Since the interleaved BIPM and PTB measurements before and after the jump constitute two coherent sets of data, the mean value of the five BIPM measurements can be directly compared to the mean of the five PTB measurements. No specific additional uncertainty component related to this instability was included in the final comparison results.

Therefore, the difference between the PTB and the BIPM was computed as the difference of the means of the measurement values provided in Table 12 and Table 13:

Relative difference PTB-BIPM: $(K2_{PTB} - K2_{BIPM}) / K2_{BIPM} = -0.7 \times 10^{-9}$

with a relative combined standard uncertainty: $u_{\text{comp}} = 2.4 \times 10^{-9}$

where u_{comp} is calculated as the root sum square of $u_{\text{BIPM}} = 2.0 \times 10^{-9}$, $u_{\text{PTB}} = 0.94 \times 10^{-9}$ and $u_{\text{Peltier}} = 1.0 \times 10^{-9}$ (estimated in section 9.2).

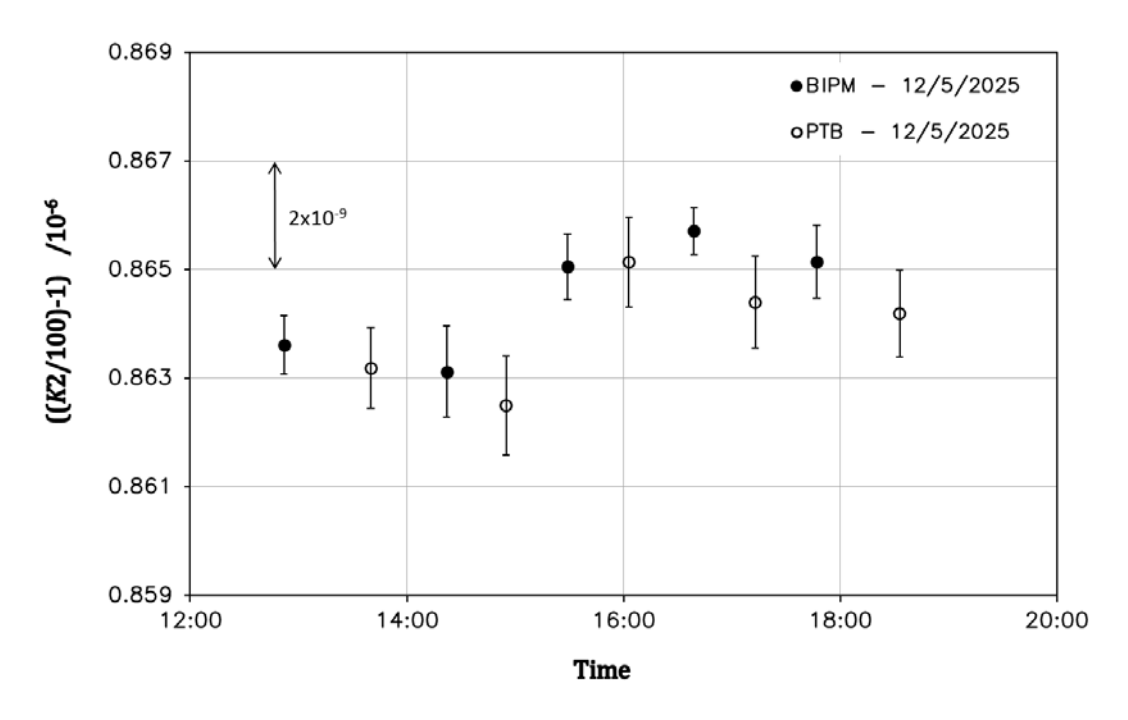


Figure 8: Measurement results for *K*2 ratio on May 12, 2025: BIPM at 1 Hz (black dots) and PTB for a 10 s cycle time (open circles). Error bars correspond to the dispersion observed for each measurement.

10. Conclusion

The on-site key comparison BIPM.EM-K12 carried out in May 2025 between the PTB and the BIPM showed a good agreement in the measurements of a conventional 100 Ω resistor in terms of the quantized Hall resistance ($R_H(2)$), and in the determination of the resistance ratios K1 (10 $k\Omega/100 \Omega$) and K2 (100 $\Omega/1 \Omega$).

The comparison results for the measurement of $R_{100\Omega}$ in terms of $R_{\rm H}(2)$ and of K1 and K2 ratios are summarized in Table 14. In the case of the comparison of $R_{100\Omega}$ in terms of $R_{\rm H}(2)$, two individual sets of results are reported in which PTB used a GaAs- or a graphene-based QHR standard as reference. Also a direct comparison between the GaAs-based QHR standard in BIPM's system and the graphene-based QHR standard in PTB's system was successfully executed.

This was the first time that a graphene-based QHRS was used for the realization of the ohm in a key comparison of the BIPM. The results presented in Table 14 show that, within the limits of the comparison uncertainty, this type of QHRS is fully equivalent to GaAs-based ones. The direct comparison between the GaAs-based QHR standard in BIPM's system and the graphene-based QHR standard in PTB's system showed agreement within about $1 \text{ n}\Omega/\Omega$. It is therefore reasonable to expect that, thanks to their simpler implementation (operated at 4.2 K and 5 T in this comparison), graphene-based QHRs will pave the way for a wider use of the quantum Hall effect by national metrology institutes and possibly even in the industry.

Since the guidelines for realizing the SI-ohm currently only apply to GaAs-based QHRS, only the results obtained for the $100~\Omega$ measurement with GaAs QHE devices will be reported on the Key Comparison Data Base (KCDB).

The results in Table 14 will also appear as Degree of Equivalence (DoE) in the BIPM KCDB. The DoE of the participating institute with respect to the reference value is given by a pair of terms: the difference D from the reference value and its combined expanded uncertainty for k=2, i.e. U=2u. The reference value of the on-going comparison BIPM.EM-K12 was chosen to be the BIPM value.

The comparison results expressed as DoEs are summarized in Table 15.

$R_{100\Omega}$ in terms of $R_{ m H}(2)$ BIPM: GaAs-based QHR PTB: GaAs-based QHR	$(R_{\text{PTB}} - R_{\text{BIPM}}) / R_{\text{BIPM}} = 0.4 \times 10^{-9}$	$u_{\rm comp} = 2.1 \times 10^{-9}$
$R_{100\Omega}$ in terms of $R_{\rm H}(2)$ BIPM: GaAs-based QHR PTB: graphene-based QHR	$(R_{\text{PTB}} - R_{\text{BIPM}}) / R_{\text{BIPM}} = 0.0 \times 10^{-9}$	$u_{\rm comp} = 2.2 \times 10^{-9}$
Relative difference graphene- based QHR vs GaAs-based QHR (direct 1:1 comparison)	$(R_{\text{graphene_PTB}} - R_{\text{GaAs_BIPM}}) / R_{\text{GaAs_BIPM}}$ $= -0.5 \times 10^{-9}$	$u_{\rm comp} = 0.8 \times 10^{-9}$
$K1 = R_{10k\Omega}/R_{100\Omega}$	$(K1_{\text{PTB}} - K1_{\text{BIPM}}) / K1_{\text{BIPM}} = -0.7 \times 10^{-9}$	$u_{\rm comp} = 2.1 \times 10^{-9}$
$K2 = R_{100\Omega}/R_{1\Omega}$	$(K2_{\text{PTB}} - K2_{\text{BIPM}}) / K2_{\text{BIPM}} = -0.7 \times 10^{-9}$	$u_{\rm comp} = 2.4 \times 10^{-9}$

Table 14: Summary of the results of the PTB-BIPM on-site comparison BIPM.EM-K12 carried out in May 2025, and associated relative standard uncertainties. The measurement of *K*2 ratio was carried out at 1 Hz by the BIPM without applying the 'dc' correction, and with a cycle time of 10 s by the PTB.

	Degree of equivalence $D/10^{-9}$	Expanded uncertainty $U/10^{-9}$
$R_{100\Omega}$ in terms of $R_{\rm H}(2)$	0.4	4.2
$K1 = R_{10k\Omega}/R_{100\Omega}$	-0.7	4.2
$K2 = R_{100\Omega}/R_{1\Omega}$	-0.7	4.8

Table 15: Summary of the comparison results expressed as degrees of equivalence (DoEs): difference from the BIPM reference value and expanded uncertainty U(k=2).

References

- [1] https://www.bipm.org/kcdb/comparison?id=430.
- [2] SI Brochure 9th edition (2019) Appendix 2, "Mise en pratique for the definition of the ampere and other electric units in the SI", https://www.bipm.org/en/publications/mises-en-pratique.
- [3] R. Goebel, N. Fletcher, B. Rolland, M. Götz, E. Pesel, "Final report on the on-going comparison BIPM.EM-K12: comparison of quantum Hall effect resistance standards of the PTB and the BIPM", *Metrologia*, 2014, **51**, 01011.
- [4] N. Fletcher, M. Götz, B. Rolland and E. Pesel, "Behavior of 1Ω resistors at frequencies below 1 Hz and the problem of assigning a dc value", *Metrologia*, 2015, **52**, 509-513.
- [5] P. Gournay, B. Rolland, J. Kučera, L. Vojáčková, P. Chrobok, "On-site comparison of quantum Hall effect resistance standards of the CMI and the BIPM", *Metrologia*, 2017, **54**, 01014.
- [6] P. Gournay, B. Rolland, C. Sanchez, "On-site comparison of quantum Hall effect resistance standards of the NRC-CNRC and the BIPM", *Metrologia*, 2019, **56**, 1A, 01002.
- [7] F. Delahaye, "DC and AC techniques for resistance and impedance measurements", *Metrologia*, 1992, **29**, 81-93.
- [8] P. Gournay, B. Rolland, Y. Lu and J. Zhao, "On-site comparison of quantum Hall effect resistance standards of the NIM and the BIPM", *Metrologia*, 2020, **57**, 1A, 01009.
- [9] F. Delahaye, T.J. Witt, F. Piquemal and G. Genevès, "Comparison of quantum Hall effect resistance standards of the BNM/LCIE and the BIPM", *IEEE Trans on Instr. and Meas.*, 1995, **44**, n°2, 258-261.
- [10] F. Delahaye and B. Jeckelmann, "Revised technical guidelines for reliable dc measurements of the quantized Hall resistance", *Metrologia*, 2003, **40**, 217-223.
- [11] F. Delahaye and D. Bournaud, "Accurate ac measurements of standard resistors between 1 and 20 Hz", *IEEE Trans on Instr. and Meas.*, 1993, **42**, n°2, 287-291.
- [12] A. Satrapinski, M. Götz, E. Pesel, N. Fletcher, P. Gournay, B. Rolland, "New Generation of Low-Frequency Current Comparators Operated at Room Temperature", *IEEE Trans. on Instr. and Meas.*, 2017, **66**, n°6, 1417-1424.
- [13] F. Delahaye, "An ac-bridge for low frequency measurements of the quantized Hall resistance", *IEEE Trans. on Instr. and Meas.*, 1991, **40**, n°6, 883-888.
- [14] M. Götz, D. Drung, E. Pesel, H.-J. Barthelmess, C. Hinnrichs, C. Aßmann, M. Peters, H. Scherer, B. Schumacher, and T. Schurig, "Improved cryogenic current comparator setup with digital current sources", *IEEE Trans. Instrum. Meas.*, 2009, **58**, 1176-1182.
- [15] D. Drung and J.-H. Storm, "Ultra-low noise chopper amplifier with low input charge injection", *IEEE Trans. Instrum. Meas.*, 2011, **60**, 2347-2352.
- [16] D. Drung, M. Götz, E. Pesel, H.-J. Barthelmess, and C. Hinnrichs, "Aspects of application and calibration of a binary compensation unit for cryogenic current comparator setups", *IEEE Trans. Instrum. Meas.*, 2013, **62**, 2820-2827.
- [17] Y. Yin, M. Kruskopf, P. Gournay, B. Rolland, M. Götz, E. Pesel, T. Tschirner, D. Momeni, A. Chatterjee, F. Hohls, K. Pierz, H. Scherer, R.J. Haug and H.W. Schumacher, "Graphene quantum Hall resistance standard

- for realizing the unit of electrical resistance under relaxed experimental conditions", *Phys. Rev. Applied*, 2025, **23**, 014025.
- [18] D.H. Chae, M. Kruskopf, J. Kucera, J. Park, N.T.M. Tran, D.B. Kim, K. Pierz, Martin Götz, Y. Yin, P. Svoboda, "Investigation of the stability of graphene devices for quantum resistance metrology at direct and alternating current", *Meas. Sci. Technol.*, 2022, **33**, 065012.
- [19] H. He, S. Lara-Avila, K.H. Kim, N. Fletcher, S. Rozhko, T. Bergsten, G. Eklund, K. Cedergren, R. Yakimova, Y. W. Park, A. Tzalenchuk and S. Kubatkin, "Polymer-encapsulated molecular doped epigraphene for quantum resistance metrology", *Metrologia*, 2019, **56**, 045004.
- [20] A.F. Rigosi, A.R. Panna, S.U. Payagala, M. Kruskopf, M.E. Kraft, G.R. Jones, "Graphene Devices for Tabletop and High-Current Quantized Hall Resistance Standards," *IEEE Trans. Instrum. Meas.*, vol. 68, no. 6, pp. 1870-1878, 2019.
- [21] M. Kruskopf and R. E. Elmquist, "Epitaxial graphene for quantum resistance metrology", *Metrologia*, 2018, **55**, R27.
- [22] N. Shetty, T. Bergsten, G. Eklund, S. Lara Avila, S. Kubatkin, K. Cedergren and H. He, "Long-term stability of molecular doped epigraphene quantum Hall standards: single elements and large arrays $(R_K/236 \approx 109 \,\Omega)$ ", *Metrologia*, 2023, **60**, 055009.
- [23] L. Callegaro, S. Bauer, B. Jeanneret, M. Kruskopf, M. Marzano, M. Ortolano, F. Overney, "Good practice guide on the graphene-based AC-QHE realization of the farad", arxiv.org/pdf/2205.04915.
- [24] P. Gournay, B. Rolland, N.H. Kaneko, T. Oe, E. Pesel, M. Götz, "Sub-Hz Frequency Dependence of New 1 Ω Standard Resistors Based on Nickel-Chromium Alloy Metal Foil Technology," *2024 Conference on Precision Electromagnetic Measurements (CPEM)*, 2024, doi: 10.1109/CPEM61406.2024.10645988.